CHALMERS
UNIVERSITY OF TECHNOLOGY

Comparison of the low noise performance of GaN HEMTs and MIS-HEMTs at cryogenic temperatures

Comparison of the low noise performance of GaN HEMTs and MIS-HEMTs at cryogenic temperatures

Mohamed Aniss Mebarki [#], Ragnar Ferrand-Drake Del Castillo [*], Erik Sundin [#], Denis Meledin [#], Mattias Thorsell [*], Niklas Rorsman [*], Victor Belitsky [#], Vincent Desmaris [#]

[#] Group for Advanced Receiver Development (GARD), Department of Space, Earth and Environment, Chalmers University of Technology, Sweden

[*] Microwave Electronics Lab (MEL), Department of Microtechnology and Nanoscience, Chalmers University of Technology, Sweden

{aniss, ragnarf, erik.sundin, denis.meledin, mattias.thorsell, niklas.rorsman, victor.belitsky, vincent.desmaris}@chalmers.se

***Abstract* — This work presents the comparison of the noise performance of AlGaN/GaN MIS-HEMTs and HEMTs at cryogenic temperatures. Wideband noise measurements at a physical temperature of ~ 4 K were performed in order to extract the noise characteristics of the devices, within the range of frequencies of 3 – 7 GHz. A DC and RF characterization of the devices are also presented to further assess their cryogenic performances. Over the measured frequency band, the results indicate that both technologies are able to present an average best noise temperature as low as 8 K. The MIS-HEMT presents a slight advantage at low bias condition, mainly due to its reduced gate capacitance. The presented results are the first report on the microwave low-noise performance of cryogenic GaN MIS-HEMT, and constitute their current state-of the art.**

***Keywords* — AlGaN/GaN, MIS-HEMT, cryogenic, LNA**

I. Introduction

The Gallium-Nitride (GaN)-based High Electron Mobility Transistors (HEMTs) combine a set of excellent microwave, high power and low-noise performances [1] [2] [3] [4], owing to the material's properties. Most recently, GaN-HEMTs featured competitive results in terms of low-noise operation at cryogenic temperatures (≤10 K) [5] [6] [7]. These latter pave the way for their potential deployment in different applications requiring an ultimate level of sensitivity and reliability at such low temperatures, mainly including the space instrumentation and quantum computing. However, compared to their III-V and SiGe counterparts, the current state of the art of the GaN-HEMTs' noise performance still presents room for improvement especially for cryogenic operation. Also, the latter works were exclusively dealing with the cryogenic noise performance of GaN-based HEMTs with Schottky gate (SG). Among the limitations of the latter, as shown in [6] [8], the Schottky gate leakage contributes with a Shot noise which calls for the investigation of other technological alternatives. As one of those, GaN Metal-Insulator-Semiconductor (MIS)-HEMTs incorporate a thin dielectric layer between the gate metal and the semiconductor barrier. When compared to the conventional HEMTs, several reports in the literature attributed to the MIS structure a decrease of the gate leakage, an enhanced large-signal performance through improving the gate reliability, a larger gate voltage swing and a higher power-handling capability [9] [10] [11]. In terms of low-noise performance, the contribution of the gate insulation to the design of low-noise amplifiers (LNAs) at room temperature was studied [12] [13].

However, to the best of the authors' knowledge, the microwave noise performance of GaN MIS-HEMTs at cryogenic temperatures have not yet been reported.

This paper presents therefore a comparative study of GaN-based MIS- and Schottky-HEMTs, focused on their microwave noise performances at cryogenic temperatures. The characteristics of the devices are measured at room temperature (RT) and the cryogenic temperature (CT) of ~4 K. Through their analysis, the results provide further insights into the promising potential of the GaN technology for cryogenic low-noise applications and possible trade-offs allowing its future improvements.

II. Device structure, measurements and Methods

The GaN-MIS-HEMTs and -HEMTs were fabricated on the same wafer, sharing the same epitaxial structure as shown in Fig. 1. Details about the processing of the structure and its characteristics were previously reported in [7]. The 0.2 µm Au/Ni/Pt-gate was obtained by e-beam lithography and evaporation. Prior to the Schottky gate formation, the top passivation layer was dry etched using NF3 by Inductive Coupled Plasma (ICP). In the case of the MIS-HEMT, a 7 nm nominally thick Si-rich SiNx layer was used as a gate dielectric by means of low-pressure chemical vapor deposition (LPCVD). The gate T-shape extends with 0.2 µm field-plates towards both the source and drain. The gate-to-source and gate-to-drain distances were respectively 0.75 µm and 1.5 µm. The tested samples featured a 2x25 µm gate-width.

The DC and RF characterization of the devices was performed on-wafer in a cryogenic probe-station at RT and CT. The DC measurements were obtained using an Agilent B1500A semiconductor parameter analyzer. The S-parameters were measured from 0.2 to 40 GHz, using a Rhode & Schwartz ZVA67 Vector Network Analyzer (VNA). The noise measurements were performed at a physical temperature of ~ 4 K within the range of frequencies of 3 – 7 GHz, using a cryogenic test setup based on the cryogenic attenuator method as described in [7]. The noise data were obtained using the Agilent MXA N9020A signal analyzer.

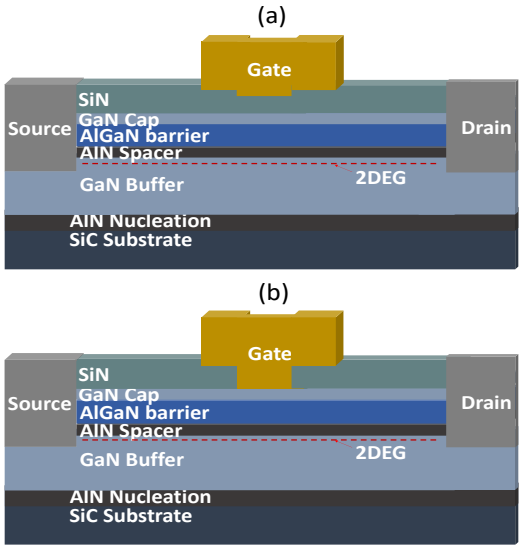

Fig. 1. Epitaxial structure of the tested sample: a) GaN-MIS-HEMT, b) -HEMT

The noise measurements and the extraction of the cryogenic noise model rely on the methods presented in [6] [7]. The minimum noise temperature, T_{min} , extracted using the cryogenic noise test setup presents a standard uncertainty of ± 0.78 K.

III. Results and Discussion

The MIS-HEMT presented a maximum drain current, I_{DS}, at V_{GS} = 1 V of 1229 and 1171 mA/mm at RT and CT. It compares to the HEMT by about 12 % and 3 % larger, at both RT and CT respectively. Comparing the variation with temperature of I_{DS}, unlike the HEMT, the saturation current of the MIS-HEMT at CT was observed to decrease even at fully opened-channel conditions. This is pointing towards the activation of a trapping effect at CT, most likely located underneath the gate as this is the only region which differs between the two samples. Such a cryogenic phenomenon was linked to the gate processing in [14], while similar behaviour was also observed in [6].

The threshold voltage at CT of the MIS-HEMT was around V_{GS} = -5 V, shifted by about +0.4 V compared to RT. The HEMT's pinch off was at -2.2 V, with only +70 mV shift compared to RT. Both samples presented a similar on-resistance, extracted from the slope of the $I_{DS}(V_{DS})$ curve, of around 0.9 Ω.mm, improving by about 45 % compared to RT. The maximum transconductance, g_{m-max}, increased upon cooling of both the MIS-HEMT and HEMT compared to RT by about 10 and 20 %. The transconductance of the MIS structure was reduced by ~ 40 % compared to the HEMT. As expected, the gate leakage decreased significantly upon the cooling of both samples as shown in Fig. 3 at different V_{DS}. While a larger difference in I_{GS} between the HEMT and MIS-HEMT could have been expected, the gate insulation might be hindered by the existence of a parallel path for the leakage. Nevertheless, the improvement of I_{GS} at low temperature is found more pronounced in the case of the MIS-HEMT.

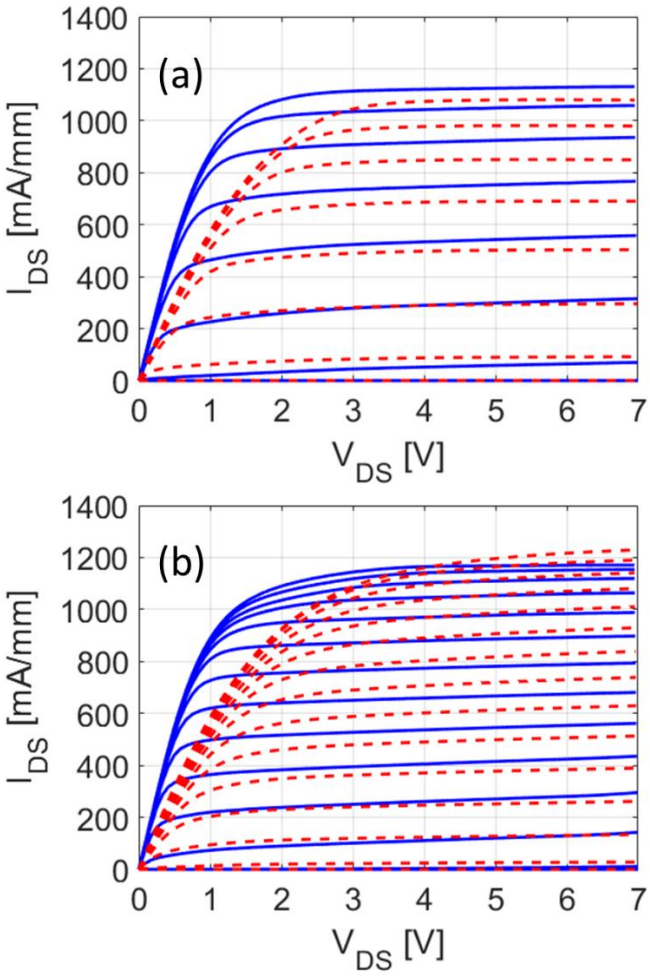

Fig. 2. $I_{DS}(V_{DS})$ characteristic at RT (red dashed lines) and CT (blue solid lines) of: a) HEMT at V_{GS} [V] = [-2.5:0.5:1], b) MIS-HEMT, at V_{GS} [V] = [-6:0.5:1].

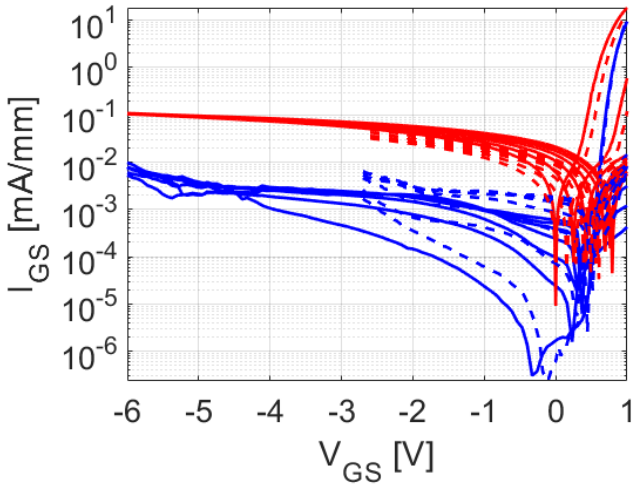

Fig. 3. $I_{GS}(V_{GS})$ characteristic of the GaN HEMT (dashed lines) and MIS-HEMT (solid lines), at V_{DS} ranging from 0 – 6 V, with steps of 1 V, at RT (red) and CT (blue).

Table 1: Summary of the DC characteristic of the HEMT and MIS-HEMT

	HEMT		MIS-HEMT	
	RT	CT	RT	CT
I_{DS-max} [mA/mm]	1079	1131	1229	1171
R_{on} [Ω.mm]	1.6	0.9	1.6	1.9
V_{TH} [V]	-2.1	-2.2	-5.4	-5
g_{m-max} [mS/mm]	430	517	271	299

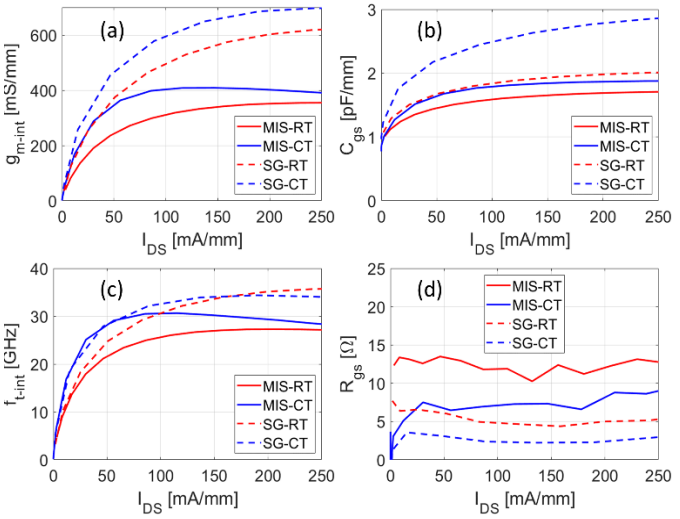

Fig. 4. The variation with I_{DS} at V_{DS} = 4 V of the intrinsic extracted small-signal parameters of the HEMT (dashed lines) and MIS-HEMT (solid lines), at RT (red) and CT (blue). a) g_{m-int}. b) C_{gs}. c) f_{t-int}. d) R_{gs}.

The DC characteristics of the two samples at RT and CT are summarized in Table 1. Their overall variation indicates an improvement of the electrical transport in both devices at CT.

The following discussion is focused on the drain voltage of V_{DS} = 4 V, as it ensures a saturation of the electron velocity in the channel while limiting the self-heating effects which is beneficial for the noise performance. As shown in (Fig. 4a – b), due to a larger effective distance between the gate and the channel, the MIS-HEMT presented a reduction of both the intrinsic transconductance, g_{m-int}, and gate capacitance, C_{gs}. Both of these parameters control the intrinsic cut-off frequency of the device, but in opposing ways. However, the rise of g_{m-int} with I_{DS} is relatively faster than that of C_{gs}.Consequently, at low I_{DS}, f_{t-int} of the MIS-HEMTs is at least equal to that of the HEMT, at both RT and CT (Fig. 4-c). As seen in Fig.4-d, the results indicate a larger intrinsic gate resistance R_{gs} in the MIS-HEMT. Since the gate metallization of both devices was obtained simultaneously using the same processing, the difference in R_{gs} might be attributed to the structure of the region underneath the gate and the presence of the dielectric in the case of the MIS-HEMT. Nevertheless, the contribution of the latter is diminished at CT since a lower difference in R_{gs} between the two samples is observed.

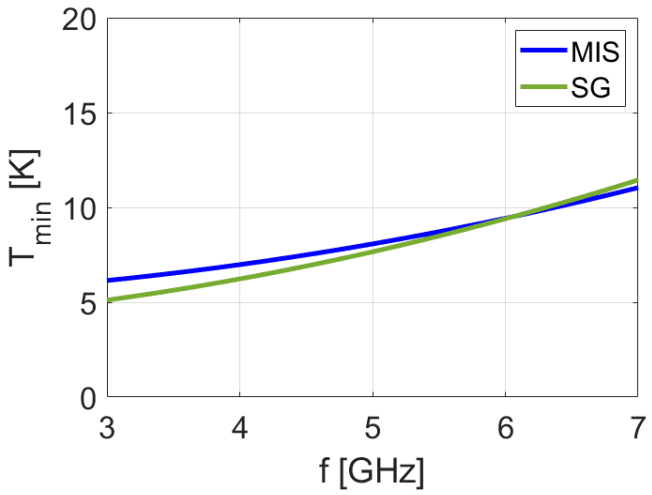

Fig. 5. Frequency dependence of T_{min} at CT of the GaN MIS-HEMT and HEMT, at the optimum-noise bias at V_{DS} [V]= 4.

Fig. 5 presents the extracted frequency dependence of the minimum noise temperature, T_{min}, at the optimum bias point of the two samples at CT, in the range of 3 – 7 GHz. Within this frequency range, the MIS-HEMT presents a similar best noise temperature of around 8 K. The optimum-noise bias was obtained at V_{DS} = 4 V around I_{DS} = 85 mA/mm and 88 mA/mm for respectively the MIS-HEMT and HEMT. Fig. 6 compares the variation with I_{DS} of the average T_{min} over the same frequency range at CT. The MIS-HEMT features a slight advantage at very low I_{DS}. This is mainly attributed to the reduced gate capacitance in the MIS-HEMT. Therefore, this gives advantage to the MIS-HEMT from the perspective of the design of low-noise amplifiers (LNAs) with low-power consumption. Higher I_{DS} leads to a faster increase of the MIS-HEMT's T_{min}, which becomes gradually larger compared to the SG-HEMT. This can be explained by the saturation of the intrinsic transconductance of the MIS-HEMT at a lower level compared to SG, while the self-heating is further limiting T_{min} at higher I_{DS} in both samples.

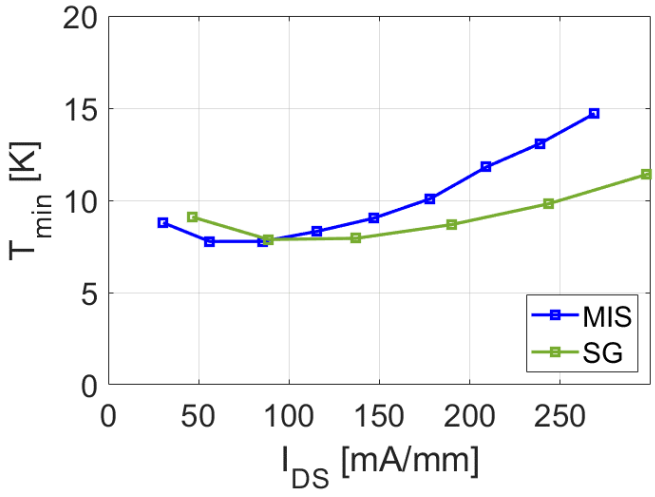

Fig. 6. Comparison of the current dependence at V_{DS} = 4 V of the extracted average T_{min} at CT of the HEMT (solid line) and MIS-HEMT (dashed line).

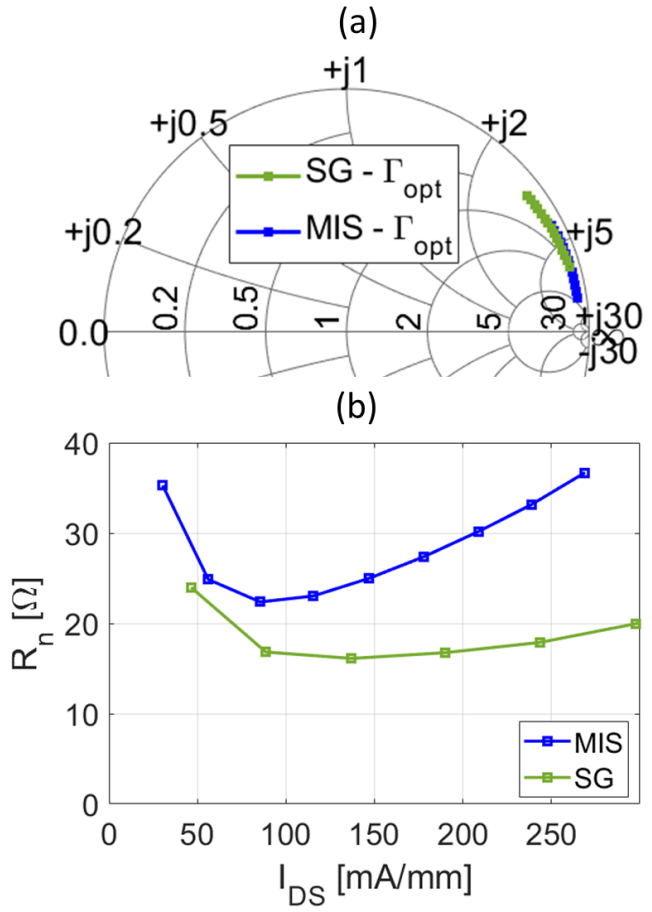

Fig. 7. a) Extracted Γ_{opt} at the optimum bias at CT of the HEMT (in green) and MIS-HEMT (in blue), from 3 to 7 GHz, considering a reference impedance Z0 = 50 Ω. b). I_{DS} dependence of R_n at CT at 5 GHz, of the MIS-HEMT (blue line) and HEMT (green line).

Completing the cryogenic noise model of both samples, Fig. 7-a – b plot respectively the optimum impedance in the Smith Chart within the frequency range of 3 to 7 GHz and the bias-dependence of the noise resistance R_n. Mainly controlled by the combined effects of R_{gs} and the transconductance, a low value of the latter is desired for the design of LNAs which gives advantage to the HEMT from that perspective.

IV. Conclusion

In conclusion, the potential of GaN-based MIS-HEMT with 0.2 µm gate length for low noise operation at cryogenic temperatures was demonstrated through the measurement and extraction of its microwave noise characteristics at 4 K. Through the comparison of the results against those obtained with a Schottky gated HEMT, despite failing to significantly reduce the gate leakage, it was revealed that the MIS-HEMT takes advantage of a lower gate capacitance which translates into a lower T_{min} at low I_{DS}. While representing the current state of the art of cryogenic GaN MIS-MEHTs' low-noise performance, these results call for future investigation of the potential of further reduction of the gate leakage, using other types of gate insulators for instance, and its impact on the noise performance at low temperatures.

References

[1] K. W. Kobayashi *et al.*, "A cool, sub-0.2 dB noise figure GaN HEMT power amplifier with 2-watt output power," *IEEE journal of solid-state circuits*, vol. 44, p. 2648–2654, 2009.

[2] V. Desmaris *et al.*, "Comparison of the DC and microwave performance of AlGaN/GaN HEMTs grown on SiC by MOCVD with Fe-doped or unintentionally doped GaN buffer layers," *IEEE Transactions on electron devices*, vol. 53, p. 2413–2417, 2006.

[3] R. Nikandish, "GaN Integrated Circuit Power Amplifiers: Developments and Prospects," *IEEE Journal of Microwaves*, vol. 3, pp. 441-452, 2023.

[4] M. Thorsell, K. Andersson, M. Fagerlind, M. Sudow, P.-A. Nilsson and N. Rorsman, "Thermal characterization of the intrinsic noise parameters for AlGaN/GaN HEMTs," in *2008 IEEE MTT-S International Microwave Symposium Digest*, 2008.

[5] V. Desmaris, D. Meledin, E. Sundin, M. Thorsell, N. Rorsman and V. Belitsky, "Characterization of GaN-based Low Noise Amplifiers at Cryogenic Temperatures," in *30th International Symposium on Space THz Technology (ISSTT2019)*, Gothenburg, Sweden, April 15-17, 2019.

[6] M. A. Mebarki *et al.*, "Noise Characterization and Modeling of GaN-HEMTs at Cryogenic Temperatures," *IEEE Transactions on Microwave Theory and Techniques*, 2022.

[7] M. A. Mebarki *et al.*, "GaN High-Electron-Mobility Transistors with Superconducting Nb Gates for Low-Noise Cryogenic Applications," *physica status solidi (a)*, p. 2200468, 2022.

[8] C. Sanabria, A. Chakraborty, H. Xu, M. J. Rodwell, U. K. Mishra and R. A. York, "The effect of gate leakage on the noise figure of AlGaN/GaN HEMTs," *IEEE electron device letters*, vol. 27, p. 19–21, 2005.

[9] Y.-S. Lin, Y.-W. Lain and S. S. H. Hsu, "AlGaN/GaN HEMTs with low leakage current and high on/off current ratio," *IEEE Electron Device Letters*, vol. 31, p. 102–104, 2009.

[10] Z. H. Liu *et al.*, "Improved linearity for low-noise applications in 0.25 µm GaN MISHEMTs using ALD Al2O3 as gate dielectric," *IEEE Electron Device Letters*, vol. 31, pp. 803-805, 2010.

[11] J. J. Freedsman, T. Kubo, S. L. Selvaraj and T. Egawa, "Suppression of Gate Leakage and Enhancement of Breakdown Voltage Using Thermally Oxidized Al Layer as Gate Dielectric for AlGaN/GaN Metal–Oxide–Semiconductor High-Electron-Mobility Transistors," *Japanese journal of applied physics*, vol. 50, p. 04DF03, 2011.

[12] S. D. Nsele, J. G. Tartarin, L. Escotte, S. Piotrowicz and S. Delage, "InAlN/GaN HEMT technology for robust HF receivers: An overview of the HF and LF noise performances," in *2015 International Conference on Noise and Fluctuations (ICNF)*, 2015.

[13] Z. H. Liu *et al.*, "High microwave-noise performance of AlGaN/GAN MISHEMTs on silicon with Al2O3 gate insulator grown by ALD," *IEEE electron device letters*, vol. 31, p. 96–98, 2009.

[14] R. Cuerdo *et al.*, "The kink effect at cryogenic temperatures in deep submicron AlGaN/GaN HEMTs," *IEEE electron device letters*, vol. 30, p. 209–212, 2009.